Peptide Design: Influence of a Guest Aib-Pro Segment on the Stereochemistry of an Oligo-Val Sequence—Solution Conformations and Crystal Structure of Boc-(Val)$_2$-Aib-Pro-(Val)$_3$-OMe

ISABELLA L. KARLE,[1] JUDITH L. FLIPPEN-ANDERSON,[1] K. UMA,[2] HEMALATHA BALARAM,[2] and P. BALARAM[2]

[1]Laboratory for the Structure of Matter, Naval Research Laboratory, Washington, D.C. 20375-5000, and
[2]Molecular Biophysics Unit, Indian Institute of Science, Bangalore 560 012, India

SYNOPSIS

The peptide Boc-Val-Val-Aib-Pro-Val-Val-Val-OMe has been synthesized to investigate the effect of introduction of a strong β-turn promoting guest segment into an oligopeptide with a tendency to form extended structures. ^{1}H-nmr studies in solution using analysis of NH group solvent accessibility and nuclear Overhauser effects suggest an appreciable solvent dependence of conformations. In chloroform a 3_{10}-helical structure is favored, while in dimethylsulfoxide an Aib-Pro β-turn with extended arms on either side is suggested. In the crystal, the backbone forms a somewhat distorted 3_{10}-helix despite the presence of a Pro residue in the middle. Among the four possible intrahelical hydrogen bonds three are of the 4 → 1 type and one 5 → 1. Head-to-tail NH···O=C hydrogen bonds link the helical molecules into continuous columns. The space group is $P2_12_12_1$ with a = 11.320(2), b = 19.889(3), and c = 21.247(3) Å.

INTRODUCTION

The design of stereochemically constrained synthetic peptide models for secondary structural elements in proteins is being explored as the first step in a modular approach to the construction of a synthetic protein mimic (for recent reports in the area of de novo protein design see Refs. 1–5). Earlier reports from our laboratories have described the characterization of peptide helices in the solid state[6–10] and in solution,[11–13] in sequences incorporating α-aminoisobutyric acid (Aib),* a residue with a very strong preference for helical conformations.[15–21] The development of disulfide cross-linked peptides as models for antiparallel β-sheet conformations has also been detailed.[22–27] The construction of acyclic models for antiparallel β-hairpins (Figure 1) is being attempted using β-turn nucleating sequences as guests, in a host peptide sequence comprised of residues with a high β-sheet potential. In this report, we describe the solution and solid state conformational analysis of the peptide Boc-Val-Val-Aib-Pro-Val-Val-Val-OMe (**1**) [Boc: (*tert*-butyloxy)-carbonyl]. The sequence was chosen in view of the known tendency of oligo-Val sequences to adopt extended conformations in solution leading to aggregated β-sheet structures[28–33] and the strong tendency of Aib-Pro sequences to facilitate β-turn formation.[34–37] The results establish that the conformational states of **1** are solvent dependent. A β-turn structure with extended arms is favored in dimethylsulfoxide solutions, while 3_{10}-helical conformations are populated in an apolar solvent like chloroform. In crystals, a helical conformation is observed, incorporating the Pro residue in the centre of the helix.

EXPERIMENTAL

Peptide **1** was synthesized by conventional solution phase procedures, purified by silica gel column

CCC 0006-3525/90/10-111433-10 $04.00
Biopolymers, Vol. 29, 1433–1442 (1990)

* For definitions of torsional angles, see Ref. 14. All chiral amino acids are of the L configuration.

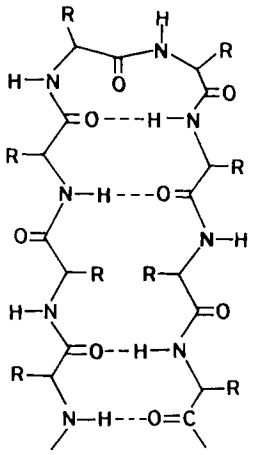

Figure 1 An antiparallel β-hairpin nucleated by a central β-turn. Dashed lines indicate intramolecular hydrogen bonds.

chromatography ($CHCl_3$-MeOH) followed by reverse-phase high performance liquid chromatography on a C_{18} column (MeOH-H_2O gradients) and fully characterized by 270-MHz ^1H- and 67.89-MHz ^{13}C-nmr.[38] All nmr studies were carried out on a Bruker WH-270 Fourier transform nmr spectrometer, as described earlier.[11,24]

X-Ray Diffraction

Crystals were grown from methanol/water solution. A diamond-shaped plate, 0.36 × 0.21 and 0.15 mm thick, mounted dry on a glass fiber was used for the collection of x-ray diffraction data at room temperature. The data were measured on an automated four-circle diffractometer using CuK_α radiation and a graphite monochromator (λ = 1.54178 Å). The $\theta - 2\theta$ scan technique was used with a 2.0° scan, a variable scan rate 3.5° to 15°/min, $2\theta_{max}$ = 115°, and hkl ranges from 0 to 12, 21, and 23, respectively. Three standard reflections monitored after every 100 measurements remained constant within 3%. A total of 3660 unique data were measured, of which 2643 had $|F|$ values greater than 3σ. Lorentz and polarization corrections were applied. The space group is $P2_12_12_1$ with cell dimensions a = 11.320(2), b = 19.889(3), c = 21.247(3) Å, V = 4783.3 Å^3, and Z = 4. The calculated density is 1.125 g cm^{-3} based on a molecular weight of 810.06 for the formula $C_{40}H_{71}N_7O_{10}$. There are no solvent molecules cocrystallized with the peptide.

The structure was solved using the random tangent procedure based on the tangent formula[39] as programmed in the SHELXTL package.[40] Full-matrix least-squares refinement using anisotropic

Table I Atomic Coordinates (× 10^4) and Equivalent Isotropic Displacement Parameters (Å^2 × 10^3)

	x	y	z	U (eq)
C(1)	5822 (18)	−2590 (13)	9661 (17)	104 (8)
C(2)	5961 (20)	−2823 (14)	10327 (15)	156 (13)
C(3)	5127 (20)	−3047 (11)	9267 (18)	169 (13)
C(4)	6957 (17)	−2455 (15)	9361 (14)	153 (12)
C(5)	4925 (13)	−1541 (11)	9187 (11)	71 (6)
O	5212 (10)	−1973 (12)	9689 (8)	90 (5)
O(0)	5134 (9)	−1678 (6)	8651 (6)	79 (4)
N(1)	4443 (9)	−974 (7)	9425 (7)	58 (4)
C$^\alpha$(1)	4067 (10)	−471 (10)	8974 (8)	61 (5)
C′(1)	5028 (12)	−176 (14)	8594 (9)	66 (5)
O(1)	4859 (7)	54 (6)	8059 (6)	73 (4)
C$^\beta$(1)	3363 (11)	59 (14)	9349 (13)	65 (6)
C$^{\gamma 1}$(1)	2250 (11)	−228 (13)	9602 (10)	77 (6)
C$^{\gamma 2}$(1)	3061 (13)	667 (12)	8916 (11)	84 (6)
N(2)	6154 (8)	−230 (8)	8812 (8)	47 (4)
C$^\alpha$(2)	7162 (10)	18 (9)	8449 (7)	47 (4)
C′(2)	7379 (11)	−408 (10)	7854 (8)	51 (5)
O(2)	8136 (8)	−188 (5)	7477 (6)	61 (3)
C$^\beta$(2)	8259 (11)	30 (9)	8881 (8)	53 (5)
C$^{\gamma 1}$(2)	8761 (12)	−672 (10)	8972 (8)	79 (6)
C$^{\gamma 2}$(2)	9216 (11)	475 (12)	8648 (9)	85 (6)
N(3)	6815 (9)	−970 (7)	7749 (7)	46 (3)
C$^\alpha$(3)	7121 (11)	−1415 (9)	7241 (8)	52 (5)
C′(3)	7395 (12)	−1070 (9)	6620 (8)	52 (5)
O(3)	8321 (7)	−1178 (5)	6349 (5)	57 (3)
C$^{\beta 1}$(3)	8192 (12)	−1842 (10)	7425 (10)	80 (6)
C$^{\beta 2}$(3)	6045 (13)	−1901 (10)	7133 (9)	79 (6)
N(4)	6601 (8)	−631 (7)	6372 (6)	47 (3)
C$^\alpha$(4)	6805 (10)	−354 (11)	5742 (8)	51 (4)
C′(4)	7821 (11)	154 (13)	5713 (12)	53 (5)
O(4)	8203 (8)	319 (6)	5188 (5)	71 (4)
C$^\beta$(4)	5634 (11)	−3 (10)	5576 (9)	75 (6)
C$^\gamma$(4)	5001 (13)	26 (15)	6185 (11)	120 (9)
C$^\delta$(4)	5441 (11)	−436 (11)	6609 (9)	78 (6)
N(5)	8201 (9)	417 (8)	6250 (7)	43 (4)
C$^\alpha$(5)	9240 (11)	846 (8)	6231 (8)	55 (5)
C′(5)	10346 (12)	454 (10)	6099 (8)	60 (5)
O(5)	11202 (8)	712 (7)	5810 (6)	85 (4)
C$^\beta$(5)	9310 (14)	1232 (10)	6898 (9)	81 (6)
C$^{\gamma 1}$(5)	8213 (16)	1614 (11)	7042 (11)	127 (9)
C$^{\gamma 2}$(5)	10436 (15)	1641 (12)	6931 (11)	133 (9)
N(6)	10416 (9)	−184 (12)	6318 (9)	71 (4)
C$^\alpha$(6)	11456 (12)	−600 (12)	6282 (11)	81 (6)
C′(6)	11515 (14)	−1129 (9)	5767 (9)	66 (6)
O(6)	12470 (8)	−1337 (8)	5605 (7)	99 (5)
C$^\beta$(6)	11637 (21)	−904 (15)	6950 (11)	200 (17)
C$^{\gamma 1}$(6)	11863 (26)	−308 (22)	7382 (18)	342 (27)
C$^{\gamma 2}$(6)	12302 (35)	−1553 (16)	7071 (17)	511 (51)
N(7)	10498 (10)	−1338 (8)	5548 (8)	61 (4)
C$^\alpha$(7)	10422 (13)	−1830 (15)	5069 (12)	55 (6)
C′(7)	9500 (14)	−1696 (10)	4601 (11)	71 (6)
O(7)	8700 (10)	−1333 (8)	4673 (7)	112 (5)
C$^\beta$(7)	10338 (14)	−2593 (19)	5342 (17)	101 (7)
C$^{\gamma 1}$(7)	9182 (16)	−2648 (11)	5633 (12)	117 (9)
C$^{\gamma 2}$(7)	10606 (19)	−3138 (13)	4953 (16)	122 (10)
O(8)	9644 (10)	−2038 (7)	4053 (7)	95 (4)
C(8)	8765 (16)	−1960 (14)	3581 (12)	146 (10)

[a] Equivalent isotropic U defined as one-third of the trace of the orthogonalized U_{ij} tensor.

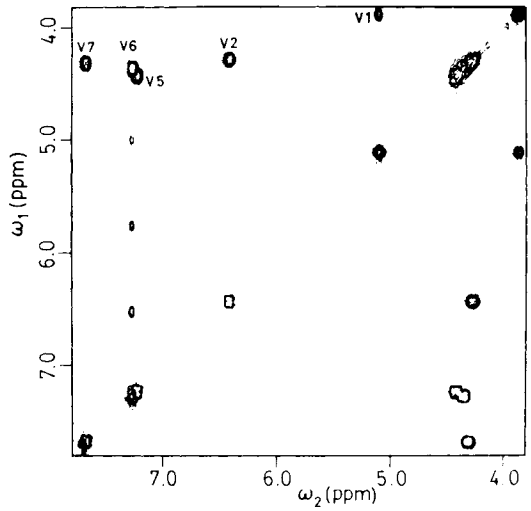

Figure 2 Contour plot of the partial two-dimensional COSY spectrum of **1** in $CDCl_3$. ω_1, ω_2 range from 3.8 to 7.8 ppm.

thermal parameters for the C, N, and O atoms (515 parameters), and ideally placed hydrogen atoms riding on the C or N atom to which they are bonded, resulted in $R = 9.5\%$ and $R_w = 4.8\%$ where $w = 1/[\sigma^2(|F|) + 0.00025\,(F_0)^2]$ for 2643 data measured $> 3\sigma$. The relatively high value for the R factor is probably due to the large rotational motions in some of the side chains, particularly in Val(6) (see Figure 6) that could not be represented well for the least-squares refinement.

Fractional coordinates for the nonhydrogen atoms are listed in Table I. Bond lengths and angles have values near to those usually observed in peptides,[41] except for an increase in the values for the N-C^{α}-C′ angles (vide infra).

RESULTS AND DISCUSSION

NMR Studies

Assignment of NH resonances of Val(1) and the Aib(3) residues was trivial in $CDCl_3$ due to the high field position of the urethane NH[11,13] and the singlet nature of the Aib NH. Solvent titration experiments in $CDCl_3$–$(CD_3)_2SO$ mixtures permitted correlation of the various NH resonances in the two solvents. Figure 2 shows a correlated spectroscopy (COSY) spectrum in $CDCl_3$. Sequence-specific $C^{\alpha}H$ and NH assignments for the Val residues at positions 2, 5, 6, and 7 were made on the basis of COSY connec-

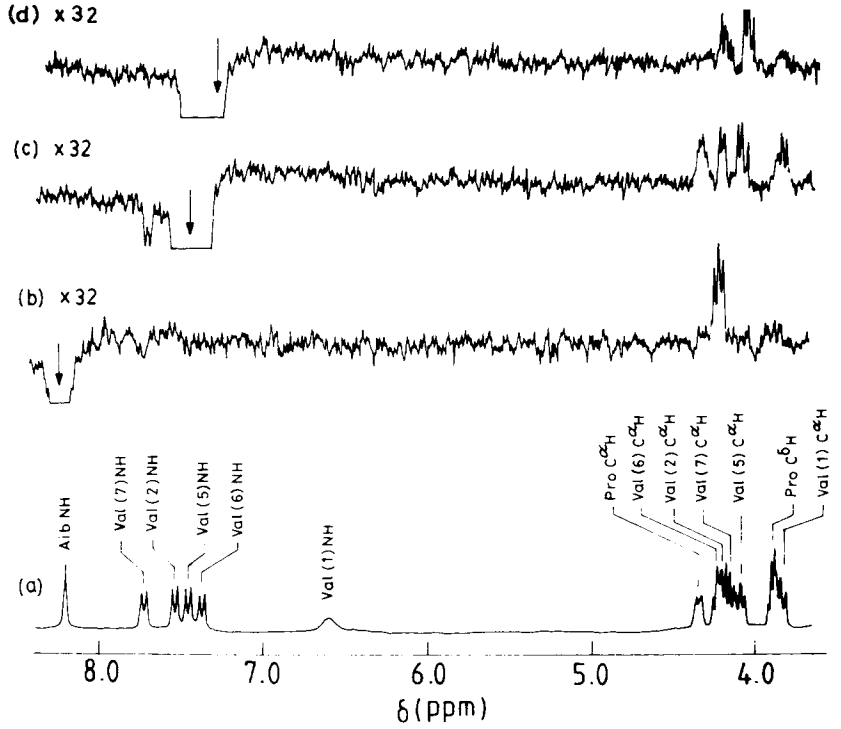

Figure 3 (a) The 270-MHz ^1H nmr spectrum of **1** in $(CD_3)_2SO$. (b)–(d). Difference NOE spectra obtained by saturation of specific NH resonances: (b) Aib(3), (c) Val(5), and (d) Val(6). Vertical scale expansions are indicated.

Table II ^{1}H-NMR Parameters for Peptide 1

Parameter	Residue						
	Val(1)	Val(2)	Aib(3)	Pro(4)	Val(5)	Val(6)	Val(7)
$\delta_{NH}(CDCl_3)$[a]	5.01	6.43	7.69	—	7.23	7.28	7.67
δ_{NH} [$(CD_3)_2SO$][a]	6.87	7.72	8.44	—	7.59	7.56	8.02
$^3J_{HNC^\alpha H}(CDCl_3)$[b]	< 4.5[c]	9.0	—	—	8.8	7.2	< 4.5[c]
$^3J_{HNC^\alpha H}$ [$(CD_3)_2SO$][b]	8.9	8.7	—	—	8.3	8.3	7.7
$\delta_{C^\alpha H}(CDCl_3)$	3.89	4.27	—	4.43	4.43	4.36	4.31
$\delta_{C^\alpha H}$ [$(CD_3)_2SO$]	3.80	4.16	—	4.30	4.09	4.23	4.14
$d\delta/dT$ [$(CD_3)_2SO$][d]	6.3	4.2	5.3	—	3.0	4.0	6.3

[a] The δ values are expressed as ppm downfield from internal $(CH_3)_4Si$, and reported for a peptide concentration of ~ 12.5 mM in both $CDCl_3$ and $(CD_3)_2SO$.
[b] Errors in J values are ~ ±0.4 Hz.
[c] These values for J are estimated from a resolution-enhanced spectrum for a broad resonance and are approximate.
[d] $d\delta/dT$ values are expressed as ppm $K^{-1} \times 10^3$.

tivities, together with the observation of $C_i^\alpha H \leftrightarrow N_{i+1}H$ interresidue NOEs in $(CD_3)_2SO$.[42] Representative difference NOE spectra are shown in Figure 3. In $CDCl_3$, NOE experiments were run at 293 K and all observed NOEs are positive. In $(CD_3)_2SO$, negligible NOEs were observed at room temperature (293 K), a feature often observed for oligopeptides in this size range, due to unfavorable correlation times, which lead to $\omega\tau_c$ values of approximately 1.[22,24] All NOEs in $(CD_3)_2SO$ were then measured at 343 K and are positive. The relevant nmr parameters for the NH and $C^\alpha H$ resonances are summarized in Table II and the NOE magnitudes obtained on irradiating various NH resonances are listed in Table III. Solvent exposure of NH groups in $CDCl_3$ was determined by paramagnetic radical broadening experiments using 2,2,6,6-tetramethyl-piperidine-1-oxyl (TEMPO) and solvent perturbation of chemical shifts in $CDCl_3$–$(CD_3)_2SO$ mixtures (Figure 4).[43] In $(CD_3)_2SO$ temperature dependence of NH chemical shifts[43] was determined over the range 293–353 K and the temperature coefficient ($d\delta/dT$) values are listed in Table II.

Solution Conformations

Addition of a polar hydrogen-bond accepting solvent like $(CD_3)_2SO$ to $CDCl_3$ solutions of **1** clearly results

Table III NOE Data for Peptide 1

Resonance Irradiated	$CDCl_3$ at 293 K		$(CD_3)_2SO$ at 343 K	
	Resonance Observed	NOE (%)	Resonance Observed	NOE (%)
Val(1)NH	Val(2)NH	1.6		
	Val(1)$C^\alpha H$	2.4	[a]	
Val(2)NH	Val(1)NH	1.4	Val(2)$C^\alpha H$	9.6
	Aib(3)NH	1.7		
	Val(1)$C^\alpha H$	1.6		
Aib(3)NH	Val(2)NH	2.9	Val(2)$C^\alpha H$	10
	Val(2)$C^\alpha H$	1.0		
Val(5)NH	[b]		Pro(4)$C^\alpha H$	5
			Val(5)$C^\alpha H$	4.2[c]
Val(6)NH[b]	Val(7)NH	1.0	Val(5)$C^\alpha H$	6.9
			Val(6)$C^\alpha H$	4.7
Val(7)NH	Val(6)NH	2	Val(6)$C^\alpha H$	12.5
			Val(7)$C^\alpha H$	3.1

[a] Urethane NH resonance broadens at high temperature and was not irradiated.
[b] Val(5) and Val(6) amide resonances overlap in $CDCl_3$.
[c] This NOE may also be a result of spillover of irradiation power onto Val(6)NH resonance.

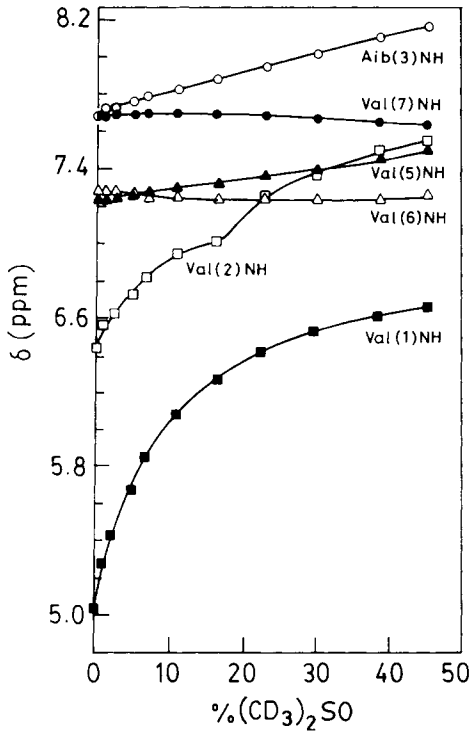

Figure 4 Solvent dependence of NH chemical shifts in **1** as a function of $(CD_3)_2SO$ concentration in $CDCl_3$–$(CD_3)_2SO$ mixtures.

in large chemical shift changes for the Val(1) and Val(2) NH resonances, indicating their solvent exposure. Of the remaining four NH groups, Val(6) and Val(7) NH resonances are perturbed only to a minor extent even up to a $(CD_3)_2SO$ concentration of ~ 20 vol %. Val(6) NH resonance shows a slight discontinuity, moving slightly downfield, after ~ 20%. Both Aib(3) and Val(5) NH resonances exhibit larger downfield shifts at higher $(CD_3)_2SO$ concentrations, suggesting partial solvent exposure. The possibility of a conformational transition induced by increasing amounts of $(CD_3)_2SO$ is emphasized by the discontinuity in the solvent titration curve for Val(2) NH. In the paramagnetic radical perturbation experiment the NH group of Val(1) is appreciably broadened even at low TEMPO concentrations, whereas the remaining five NH groups are much less affected (data not shown). These results clearly favor conformations, in $CDCl_3$, which contain four solvent-shielded NH groups, viz. Aib(3), Val(5), Val(6), and Val(7). A largely 3_{10}-helical conformation involving a succession of 4 → 1 hydrogen-bonded type III β-turns, is then consistent with the nmr data and the known stereo-chemical propensities of Aib peptides.[15-21] The continuous chain of helical hydrogen bonds is interrupted by the Pro(4) residue. However, evidence for the incorporation of Pro residues into peptide helices has been presented from nmr[44,45] and theoretical studies[46] of $(Aib\text{-}Pro)_n$ sequences, and also demonstrated in the solid state in a 16-residue synthetic peptide, where as many as three Pro residues adopt ϕ,ψ values in the helical region.[47] Further support for population of helical conformations for peptide **1** in $CDCl_3$ comes from the observation of several interresidue $N_iH \leftrightarrow N_{i+1}H$ NOEs (Table III), characteristic of ϕ,ψ values in the helical region.[42,48,49] A complete tracing of the helical backbone through successive interresidue $N_iH \leftrightarrow N_{i+1}H$ NOEs was precluded by overlap of the Val(5) and Val(6) NH protons. The expected NOE between one of the Pro $C^{\delta}H_2$ protons and the Aib(3) and Val(5) NH groups could not be detected. However, it may be emphasized that under experimental conditions used, NOE magnitudes were small and limited sensitivity precluded clear detection of effects smaller than ~ 1%.

In $(CD_3)_2SO$, the Val(5) NH exhibits a relatively low $d\delta/dT$ value (0.003 ppm/K) and also has a minimal change in chemical shift on going from $CDCl_3$ to $(CD_3)_2SO$ ($\Delta\delta$ = 0.36 ppm). This suggests that the type III Aib-Pro β-turn, stabilized by a Val(2) CO—HN Val(5) hydrogen bond is maintained in $(CD_3)_2SO$. Temperature coefficient values also point to a limited degree of solvent shielding for the Val(2) and Val(6) NH groups, while the remaining three NH groups appear exposed in $(CD_3)_2SO$. A significant feature of the NOE data in this solvent is the observation of a succession of $C_i^{\alpha}H \leftrightarrow N_{i+1}H$ NOEs for the entire segment except

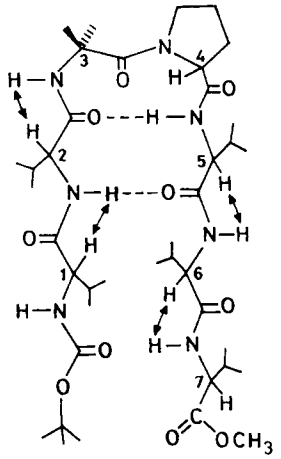

Figure 5 Proposed conformation for **1** in $(CD_3)_2SO$. Dashed lines represent hydrogen bonds and double-headed arrows represent the observed NOEs supportive of this conformation. Note that orientations of blocking groups at N and C termini are not determined.

for the Aib-Pro region, where an NH group is lacking. The magnitudes of these interresidue NOEs are large (> 5%) and in all cases they are significantly greater than the corresponding intraresidue $C_i^{\alpha}H \leftrightarrow N_{i+1}H$ NOEs. These observations strongly suggest that the interresidue ($d_{\alpha N}$) distance is shorter than the corresponding intraresidue distance, a feature indicative of ψ values of 120° ± 60°, characteristic of extended conformations.[42,48,49] The $J_{HNC^{\alpha}H}$ values in $(CD_3)_2SO$ are large (> 8 Hz) for all residues with the exception of the C-terminal Val(7) NH group. The large J values,[50] together with the NOE results, strongly favor extended structures in the β-strand region ($\phi \sim -120° \pm 30°$, $\psi \sim 120° \pm 30°$), for the Val(1), Val(2), Val(5), and Val(6) residues. A conformation consistent with the nmr results in $(CD_3)_2SO$ is illustrated in Figure 5. While the proposed structure accounts for the solvent-shielded character of the Val(5) and Val(2) NH protons, the observed NOEs and J values, alternative conformations may also be populated involving a degree of shielding of the Val(6) NH group. Candidate structures could involve a Pro-Val β-turn, with a Aib CO—HN Val(6) 4 → 1 hydrogen bond. Such a structure is also supported by an NOE (5%) between Pro $C^{\alpha}H$ and Val(5) NH, which is suggestive of $\psi_{Pro} \sim 120°$, a value in accordance with Pro occupying the $i + 1$ position of a type II β-turn. The expected hydrogen bond in the idealized antiparallel hairpin structure between Boc CO and Val(7) NH does not appear to be present in solution. This is suggestive of a fraying of the ends of the hairpin structure, due to the strongly solvating character of $(CD_3)_2SO$. In fact, temperature dependence and NOE studies in 5–10% $(CD_3)_2SO$–$CDCl_3$ mixtures indicate that even a very small amount of $(CD_3)_2SO$ is enough to break the intramolecular hydrogen bonds characteristic of a helix, resulting in conformations similar to those obtained in pure $(CD_3)_2SO$ (data not shown).

Crystal Structure

Helical Backbone. The most fascinating feature of the molecular structure is the existence of a helical backbone, despite the presence of a Pro residue in the middle of a short peptide. Figure 6 displays two different representations of the peptide as viewed

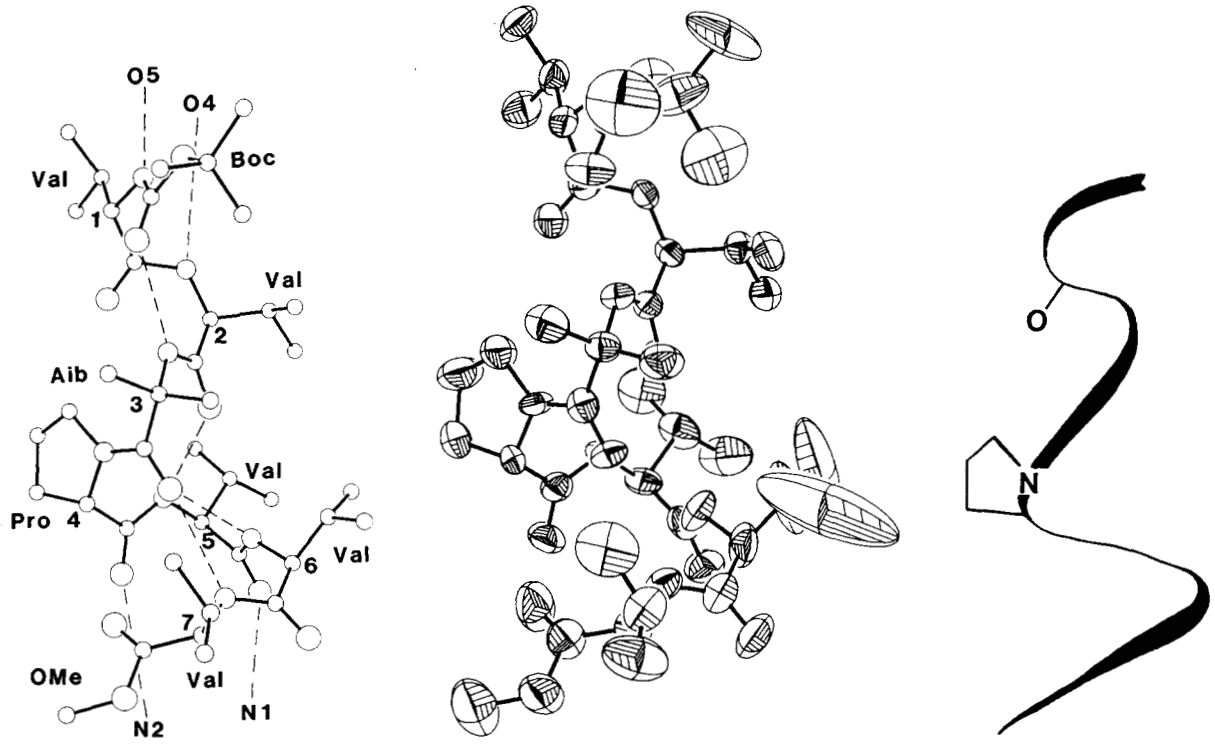

Figure 6 Three representations of the helical Boc-Val-Val-Aib-Pro-Val-Val-Val-OMe molecule in crystals, each in the same orientation. (a) Drawn by computer using coordinates determined experimentally by x-ray diffraction. The C^{α} atoms are labeled 1–7. The dashed lines represent intramolecular and head-to-tail hydrogen bonds. (b) The anisotropic thermal parameters for the C, N, and O atoms are represented by ellipsoids at the 50% level. The side chain in Val(6) shows particularly large displacements. (c) A ribbon outline of the backbone.

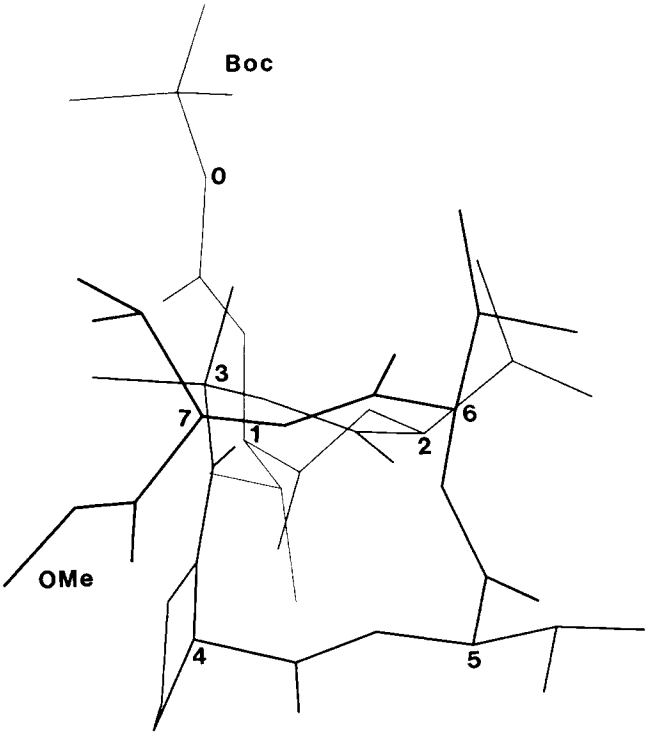

Figure 7 A view into the helix, from the bottom, that is, the OMe terminus. The C^{α} atoms are labeled 1–7.

perpendicular to the helix. Figure 7 shows the view looking into the helix from the bottom, i.e., from the OMe terminal. In Figure 7, $C^{\alpha}(2)$ and $C^{\alpha}(6)$ are nearly superimposed, as are $C^{\alpha}(3)$ and $C^{\alpha}(7)$.

The ϕ and ψ angles, shown in Table IV, attest to a distorted right-handed helix despite the absence of a proton on the N atom in the Pro residue that disturbs the hydrogen-bonding scheme. All six NH moieties available for hydrogen bonding do form strong hydrogen bonds with good geometries (Table V). Intrahelical hydrogen bonds N(3)···O(0), N(5)···O(2), and N(6)···O(3) are of the 4 → 1 type that are found in 3_{10}-helices. The final hydrogen bond in the helix is a 5 → 1 type between N(7) and O(3). The N(1)H and N(2)H groups form head-to-tail hydrogen bonds with O(5) and

Table IV Conformational Angles[a] (deg)[b]

	1 Val	2 Val	3 Aib	4 Pro	5 Val	6 Val	7 Val
ϕ(N — C^{α})	−64[c]	−69	−42	−71	−71	−101	−140
ψ(C^{α} — C′)	−20	−8	−53	−17	−33	−24	161[d]
ω(C′ — N)	177	−171	−173	174	−174	180	177[e]
χ^1	−66	77		13	−56	−63	70
	173	−160			−175	156	−161
χ^2				−20			
χ^3				18			
χ^4				−8			
$C^{\delta}NC^{\alpha}C^{\beta}$				−4			

[a] ESDs ~ 1.5°.

[b] The torsion angles for rotation about bonds of the peptide backbone (ϕ, ψ, and ω) and about bonds of the amino acid side chains (χ) are described in Ref. 14.

[c] C′(0)N(1)C^{α}(1)C′(1) where C′(0) is part of Boc.

[d] N(7)C^{α}(7)C′(7)O(8) where O(8) is part of OMe.

[e] C^{α}(7)C′(7)O(8)C(8) where O(8) and C(8) are part of OMe.

Table V Hydrogen Bonds

Type	Donor	Acceptor	Length (Å)		Angles (deg)	
			N···O	H···O	C=O···N	O···HN
Head to tail	N(1)	O(5)[a]	3.077	2.13[b]	110	169
	N(2)	O(4)[a]	3.018	2.15	160	149
Intramolecular						
4 → 1	N(3)[c]	O(0)	3.046	2.13	128	159
4 → 1	N(5)	O(2)	2.872	2.08	138	138
4 → 1	N(6)	O(3)	3.089	2.31	124	137
5 → 1	N(7)	O(3)	3.011	2.13	173	152

[a] With symmetry operation 1.5 − x, −y, 0.5 + z for coordinates listed in Table I.
[b] Hydrogen atoms placed in idealized positions with N—H = 0.96 Å and X—N—H angles near 120°.
[c] Atom O(1) is at 3.080 Å from N(3) but the existence of a 3 → 1 is very unlikely since the N(3)H···O(1) distance is 2.72 Å and the C=O(1)···N(3) angle is only 81°. Atoms O(6) and O(7) do not participate in any hydrogen bonding.

O(4), respectively, in an adjacent molecule related by a twofold screw. Carbonyl oxygens O(6) and O(7) do not participate in any hydrogen bonding. Carbonyl O(1), which would normally act as an acceptor from an N(4)H group in a 3_{10}-helix, cannot do so since N(4) is a part of the Pro residue. The N(4)···O(1) distance has been increased to 4.31 Å. Even though the N(3)···O(1) distance is only

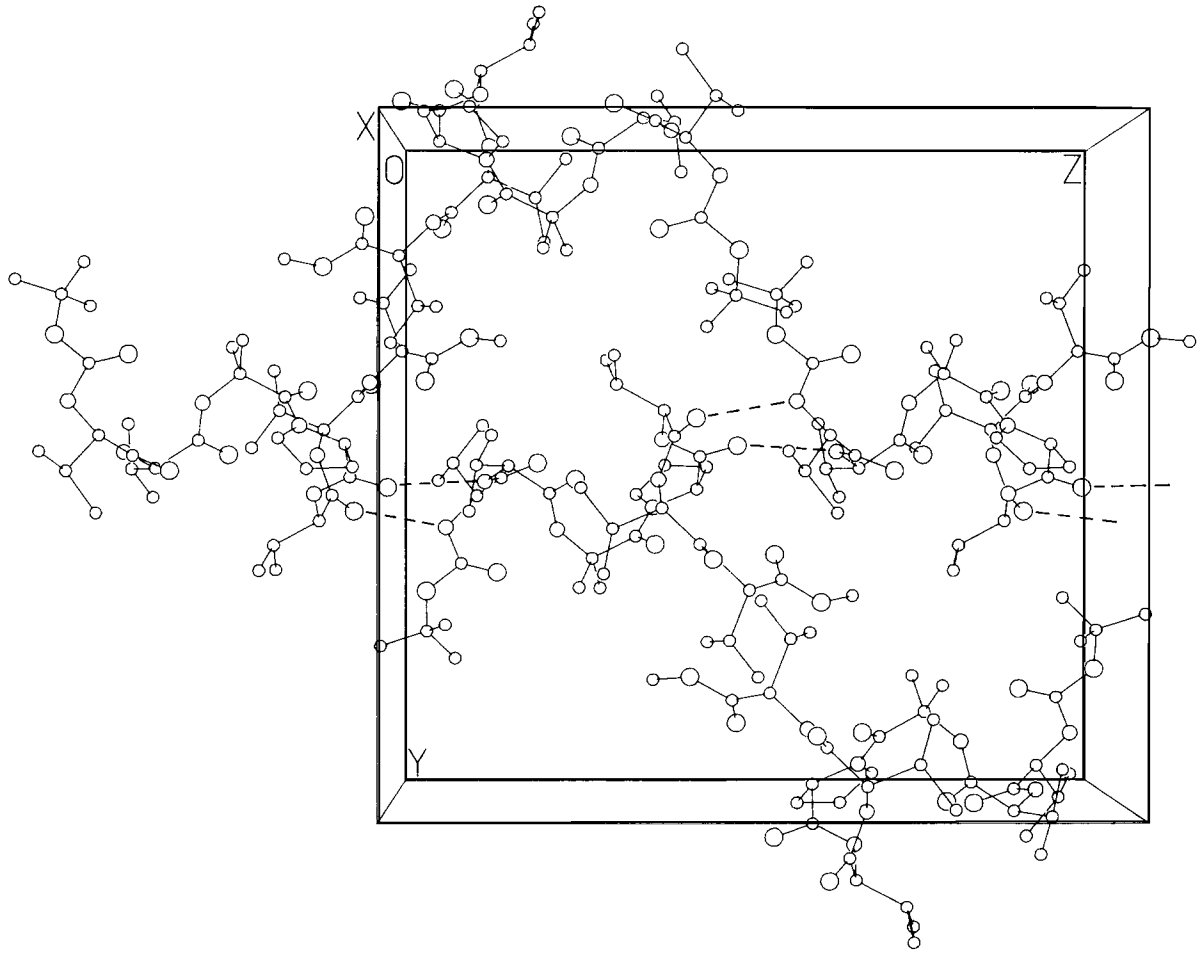

Figure 8 Crystal packing viewed down the x axis of the unit cell. Dashed lines represent head-to-tail hydrogen bonding. Hydrogen atoms have been omitted in all the diagrams.

3.080 Å, the existence of a 3 → 1 type hydrogen bond is very unlikely since the H···O(1) distance in question is 2.72 Å, a distance that is 0.4 Å larger than any H···O distance in Table V and 0.5 Å larger than H···O distances observed for 3 → 1 hydrogen bonds in other molecules, such as cyclic tetrapeptides and pentapeptides.[52]

Although the Pro residue is generally considered a helix breaker,[53] there are a few instances where Pro is incorporated into a helix in protein and peptide structures.[47,54,55] The presence of one Aib residue appears to be sufficient to overcome the helix-breaking tendency of a Pro residue.

A departure from usually observed values for the N-C^{α}-C′ angles, 111.1° average value,[41] is exhibited by an average value of 114.2° in the present heptapeptide. There is no apparent reason for the enlargement of these angles. For the Aib(3) residue in the present peptide, angle N-C^{α}-C′ = 115.0°, close to the 114.2° average. By comparison, in a 16-residue helical peptide that contains three Aib-Pro segments,[47] the values for the N-C^{α}-C′ angle of the Aib residues are 111.1°, 111.3°, and 109.9°.

Crystal Packing. The helical molecules associate into an infinite column by head-to-tail NH···O=C hydrogen bonding. Three peptide molecules in such a column, related by a twofold screw operation, are shown along the center of the cell in Figure 8, parallel to the z axis. These columns pack antiparallel to each other with hydrophobic contacts between the side groups. The open spaces that may appear to be voids in the packing (toward the upper left and lower right corners in Figure 8) are actually filled with H atoms on the many methyl groups directed into these spaces. In these areas, the nearest intermolecular approaches are $C^{\gamma 1}(5)\cdots C^{\beta 2}(3)$ = 3.66 Å and $C(8)\cdots C^{\gamma 2}(6)$ = 3.66 Å, which are quite normal values.

CONCLUDING REMARKS

The results presented above suggest that the conformational states of peptide **1** are strongly solvent dependent, with helical structures favored in $CDCl_3$ and conformations involving a central Aib-Pro β-turn with extended N- and C-terminal segments being populated in $(CD_3)_2SO$. The helical conformation of this sequence has been unambiguously characterized in crystals. The initial intention of designing a stereochemically rigid model for an antiparallel β-hairpin structure has not been realized. Nevertheless, the study has provided some insight into the effect of introducing β-turn nucleating sequences into a strong β-sheet forming sequence. Clearly, even the introduction of a single Aib residue facilitates helical folding in an otherwise poor helix-forming sequence. This is particularly important in apolar media, where cooperative intramolecular hydrogen-bond formation may provide a significant means of stabilization. The β-turn segment chosen in this study (Aib-Pro) is constrained to adopt type I (III) structures.[34-37] However, an analysis of hairpin structures in proteins that appeared subsequent to the synthesis of peptide **1** suggests that ideal hairpins with minimal fraying of the antiparallel strands may be better achieved with nucleating sequences forming type I′ or II′ β-turns.[56] The synthesis of an analogue peptide incorporating D-Pro instead of L-Pro is in progress. The crystallization of acyclic oligopeptides in the size range 6–20 residues in a form suitable for x-ray diffraction is relatively rare, for sequences containing the normal repertoire of amino acids found in proteins. Introduction of Aib residues greatly promotes crystallization, presumably by limiting the range of conformational excursions possible. It is particularly pertinent that a single Aib residue facilitates single crystal formation in the case of a helical nonapeptide presently under refinement, Boc-Val-Ala-Leu-Phe-*Aib*-Val-Ala-Leu-Phe-OMe.

This research was supported in part by the Office of Naval Research, by NIH Grant GM30902 and in part by a grant from the Department of Science and Technology, India. KU is the recipient of a fellowship from the Council of Scientific and Industrial Research, India.

Supplementary Material Available. Tables of anisotropic thermal parameters for the C, N, and O atoms, coordinates for the H atoms, bond lengths, and bond angles (pages); observed and calculated structure factors (pages). Ordering information is given on any current masthead page.

REFERENCES

1. Richardson, J. S. & Richardson, D. C. (1987) in *Protein Engineering,* Oxender, D. L. & Fox, C. F., Eds., Alan R. Liss, New York, pp. 149–163.
2. Ho, S. P. & De Grado, W. F. (1987) *J. Am. Chem. Soc.* **109,** 6751–6758.
3. Regan, L. & De Grado, W. F. (1988) *Science* **241,** 976–978.
4. Mutter, M. (1988) *Trends Biochem. Sci. (Pers. Ed.),* **13,** 260–265.
5. Urry, D. W. (1988) *Res. Develop.* **30,** 72–76.
6. Karle, I. L., Flippen-Anderson, J. L., Uma, K. & Balaram, P. (1988) *Proc. Natl. Acad. Sci. USA* **85,** 299–303.
7. Karle, I. L., Flippen-Anderson, J. L., Uma, K. & Balaram, P. (1988) *Int. J. Peptide Protein Res.* **32,** 536–543.

8. Karle, I. L., Flippen-Anderson, J. L., Uma, K., Balaram, H. & Balaram, P. (1989) *Proc. Natl. Acad. Sci. USA* **86,** 765–769.
9. Francis, A. K., Vijayakumar, E. K. S., Balaram, P. & Vijayan, M. (1985) *Int. J. Peptide Protein Res.* **26,** 214–223.
10. Karle, I. L., Flippen-Anderson, J. L., Sukumar, M. & Balaram, P. (1988) *Int. J. Peptide Protein Res.* **31,** 567–576.
11. Vijayakumar, E. K. S. & Balaram, P. (1983) *Biopolymers* **22,** 2133–2140.
12. Vijayakumar, E. K. S., Sudha, T. S. & Balaram, P. (1984) *Biopolymers* **23,** 877–886.
13. Balaram, H., Sukumar, M. & Balaram, P. (1986) *Biopolymers* **25,** 2209–2223.
14. IUPAC-IUB Commission on Biochemical Nomenclature (1970) *Biochemistry* **9,** 3471–3479.
15. Marshall, G. R. & Bosshard, H. E. (1972) *Circ. Res. Suppl.* **30/31,** 143–150.
16. Toniolo, C., Bonora, G. M., Bavoso, A., Benedetti, E., Di Blasio, B., Pavone, V. & Pedone, C. (1983) *Biopolymers* **22,** 205–215.
17. Prasad, B. V. V. & Balaram, P. (1984) *CRC Crit. Revs. Biochem.* **16,** 307–347.
18. Nagaraj, R. & Balaram, P. (1981) *Acc. Chem. Res.* **14,** 356–362.
19. Bosch, R., Jung, G., Schmitt, H. & Winter, W. (1985) *Biopolymers* **24,** 961–978.
20. Bosch, R., Jung, G., Schmitt, H. & Winter, W. (1985) *Biopolymers* **24,** 979–999, and references cited therein.
21. Bavoso, A., Benedetti, E., Di Blasio, B., Pavone, V., Pedone, C., Toniolo, C., Bonora, G. M., Formaggio, F. & Crisma, M. (1988) *J. Biomol. Struct. Dynam.* **5,** 803–817.
22. Kishore, R., Kumar, A. & Balaram, P. (1985) *J. Am. Chem. Soc.* **107,** 8019–8023.
23. Kishore, R., Raghothama, S. & Balaram, P. (1987) *Int. J. Peptide Protein Res.* **29,** 381–391.
24. Kishore, R., Raghothama, S. & Balaram, P. (1987) *Biopolymers* **26,** 873–891.
25. Karle, I. L., Kishore, R., Raghothama, S. & Balaram, P. (1988) *J. Am. Chem. Soc.* **100,** 1958–1963.
26. Karle, I. L., Flippen-Anderson, J. L., Kishore, R. & Balaram, P. (1989) *Int. J. Peptide Protein Res.* **34,** 37–41.
27. Uma, K., Balaram, H., Raghothama, S. & Balaram, P. (1988) *Biochem. Biophys. Res. Commun.* **151,** 153–157.
28. Balcerski, J. S., Pysh, E. S., Bonora, G. M. & Toniolo, C. J. (1976) *J. Am. Chem. Soc.* **98,** 3470–3473.
29. Baron, M. H., DeLoze, C., Toniolo, C. & Fasman, G. D. (1978) *Biopolymers* **17,** 2225–2239.
30. Baron, M. H., DeLoze, C., Toniolo, C. & Fasman, G. D. (1979) *Biopolymers* **18,** 411–424.
31. Bonora, G. M., Palumbo, M., Toniolo, C. & Mutter, M. (1979) *Makromol. Chem.* **180,** 1293–1304.
32. Toniolo, C., Bonora, G. M. & Mutter, M. (1979) *J. Am. Chem. Soc.* **101,** 450–454.
33. Toniolo, C., Bonora, G. M. & Salardi, C. (1981) *Int. J. Biol. Macromol.* **3,** 377–383.
34. Shamala, N., Nagaraj, R. & Balaram, P. (1977) *Biochem. Biophys. Res. Commun.* **79,** 292–298.
35. Prasad, B. V. V., Shamala, N., Nagaraj, R., Chandrasekharan, R. & Balaram, P. (1979) *Biopolymers* **18,** 1635–1646.
36. Nagaraj, R., Shamala, N. & Balaram, P. (1979) *J. Am. Chem. Soc.* **101,** 16–20.
37. Prasad, B. V. V. & Balaram, P. (1983) in *Conformation in Biology,* Srinivasan, R. & Sarma, R. H., Eds., Adenine Press, New York, pp. 133–140.
38. Balaram, H. (1984) Doctoral thesis, Indian Institute of Science, India.
39. Karle, J. & Hauptman, H. (1956) *Acta Crystallogr.* **9,** 635–651.
40. Sheldrick, G. M. (1981) *SHELXTL, An Integrated System for Solving, Refining and Displaying Crystal Structures from Diffraction Data,* University of Gottingen, Gottingen, FRG.
41. Benedetti, E. (1977) in *Peptides: Proceedings of the Fifth American Peptide Symposium;* Goodman, M. & Meienhofer, J., Eds., John Wiley & Sons, New York, pp. 257–279.
42. Wüthrich, K. (1986) *NMR of Proteins and Nucleic Acids,* Wiley, New York.
43. Wüthrich, K. (1976) *NMR in Biological Research. Peptides and Proteins,* North Holland, Amsterdam.
44. Venkatachalapathi, Y. V. & Balaram, P. (1981) *Biopolymers* **20,** 1137–1145.
45. Nagaraj, R. & Balaram, P. (1981) *Biochemistry* **20,** 2828–2835.
46. Prasad, B. V. V. & Balaram, P. (1982) *Int. J. Biol. Macromol.* **4,** 99–102.
47. Karle, I. L., Flippen-Anderson, J. L., Sukumar, M. & Balaram, P. (1987) *Proc. Natl. Acad. Sci. USA* **84,** 5087–5091.
48. Shenderovich, M. D., Nikiforovich, G. V. & Chipens, G. I. (1984) *J. Magn. Reson.* **59,** 1–12.
49. Ramakrishnan, C., Sukumar, M. & Balaram, P. (1987) *Biochem. Biophys. Res. Commun.* **149,** 953–959.
50. Kishore, R. & Balaram, P. (1984) *J. Chem. Soc. Chem. Commun.* 778–779.
51. Pardi, A., Billeter, M. & Wüthrich, K. (1984) *J. Mol. Biol.* **180,** 741–751.
52. Karle, I. L. (1978) *J. Am. Chem. Soc.* **100,** 1286–1289.
53. Chou, P. Y. & Fasman, G. D. (1974) *Biochemistry* **13,** 222–245.
54. Richardson, J. S. (1981) *Adv. Protein Chem.* **34,** 167–339.
55. Terwilliger, T. C. & Eisenberg, D. (1982) *J. Biol. Chem.* **257,** 6016–6022.
56. Sibanda, B. L. & Thornton, J. M. (1985) *Nature* **316,** 170–174.

Received July 3, 1989
Accepted September 8, 1989